

Supplemental information for:

Antitumor substitution-inert polynuclear platinum complexes stabilize G-quadruplex DNA and suppress G-quadruplex-mediated gene expression

Jaroslav Malina,^a Hana Kostrhunova,^a Nicholas P. Farrell^b and Viktor Brabec^{*a}

¹Czech Academy of Sciences, Institute of Biophysics, Kralovopolska 135, CZ-61265 Brno, Czech Republic and

²Virginia Commonwealth University, Department of Chemistry, Richmond, VA 23284-2006, USA

Table of Contents

Supplementary Figures	S3
Autoradiograms of 12% denaturing PAA gels for the <i>Taq</i> DNA polymerase stop assay on the templates containing <i>c-myc</i> , <i>c-kit2</i> , and <i>hTelo</i> G4-forming sequences in the presence of III-VI (Fig. S1)	S3
Autoradiogram of 12% denaturing PAA gel for the <i>Taq</i> DNA polymerase stop assay on the template containing <i>hTelo</i> G4-forming sequence in the presence of I and II (Fig. S2)	S4
Autoradiograms of 12% denaturing PAA gels for the <i>Taq</i> DNA polymerase stop assay on the <i>c-myc</i> ctrl template in the presence of III-VI (Fig. S3)	S5
Fluorescence melting curves for the fluorescent labeled <i>c-myc</i> G4 in 4 mM potassium phosphate buffer (pH7) and in the presence of 0.8 μM I-VI and various concentrations of competitor duplex (Fig. S4)	S6
Fluorescence melting curves for the fluorescent labeled <i>c-kit2</i> G4 in 4 mM potassium phosphate buffer (pH7) and in the presence of 0.8 μM I-VI and various concentrations of competitor duplex (Fig. S5)	S7
Fluorescence melting curves for the fluorescent labeled <i>hTelo</i> G4 in 4 mM potassium phosphate buffer (pH7) and in the presence of 0.8 μM I-VI and various concentrations of competitor duplex (Fig. S6)	S8
Fluorescence melting curves for the fluorescent labeled <i>c-myc</i> G4 in 10 mM potassium phosphate buffer (pH7) and 10 mM KCl in the presence of 0.8 μM I-VI and various concentrations of competitor duplex (Fig. S7)	S9
Fluorescence melting curves for the fluorescent labeled <i>c-kit2</i> G4 in 10 mM potassium phosphate buffer (pH7) and 10 mM KCl in the presence of 0.8 μM I-VI and various concentrations of competitor duplex (Fig. S8)	S10
Fluorescence melting curves for the fluorescent labeled <i>hTelo</i> G4 in 10 mM potassium phosphate buffer (pH7) and 10 mM KCl in the presence of 0.8 μM I-VI and various concentrations of competitor duplex (Fig. S9)	S11
CD spectra of <i>c-myc</i> G4 in the presence of II-VI (Fig. S10)	S12
	S1

CD spectra of <i>c-kit2</i> G4 in the presence of II-VI (Fig. S11)	S13
CD spectra of <i>hTelo</i> G4 in the presence of II-VI (Fig. S12)	S14
Fluorescence response of <i>c-myc</i> G4 mixed with Hoechst 33258 or thiazole orange in the presence of increasing concentrations of I-VI (Fig. S13)	S15
Antiproliferative effects of the investigated SI-PPCs (Table S1)	S15

Supplementary Figures

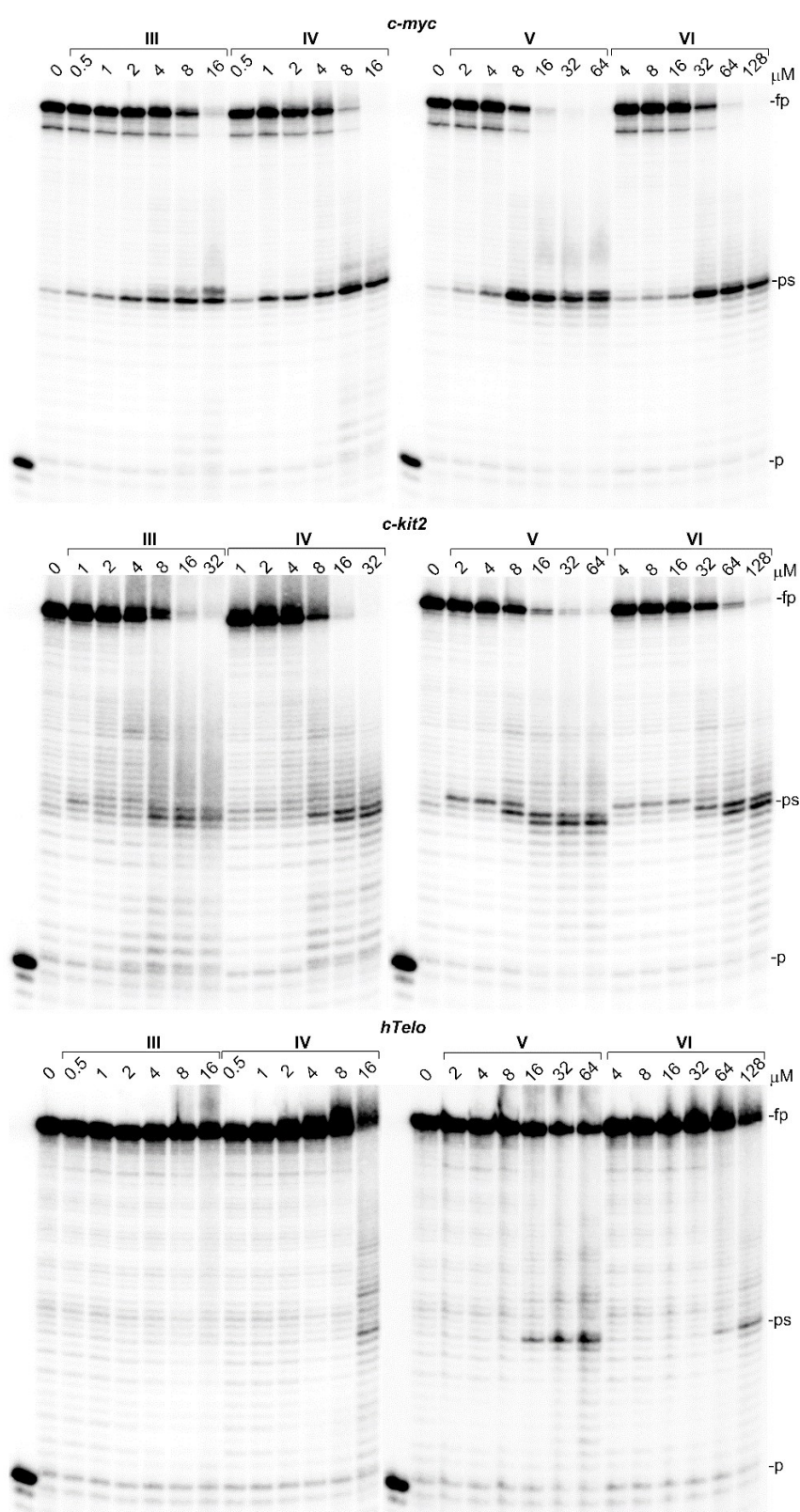


Fig. S1. Autoradiograms of 12% denaturing PAA gels for the *Taq* DNA polymerase stop assay on the templates containing *c-myc*, *c-kit2*, and *hTelo* G4-forming sequences in the presence of increasing concentrations of **III-VI**. *p*, *ps*, and *fp* correspond to primer, pausing site, and full-length product, respectively.

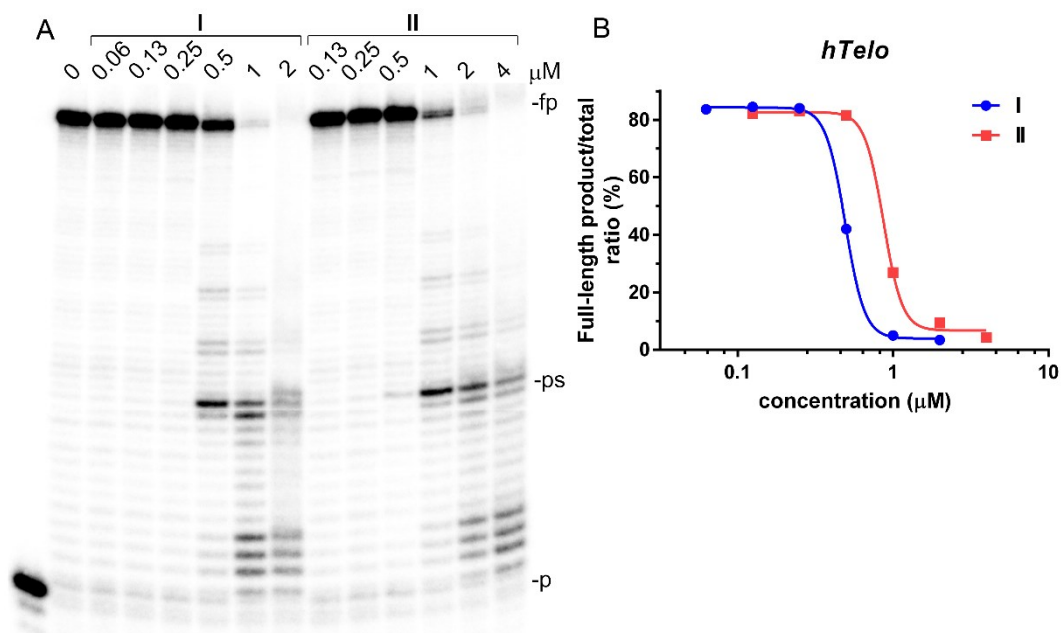


Fig. S2. (A) Autoradiogram of 12% denaturing PAA gel for the *Taq* DNA polymerase stop assay on the template containing *hTelo* G4-forming sequence with increasing concentrations of **I** and **II**. *p*, *ps*, and *fp* correspond to primer, pausing site, and full-length product, respectively (B) Graphical representation of the full-length product synthesis in the presence of increasing concentrations of **I** and **II**.

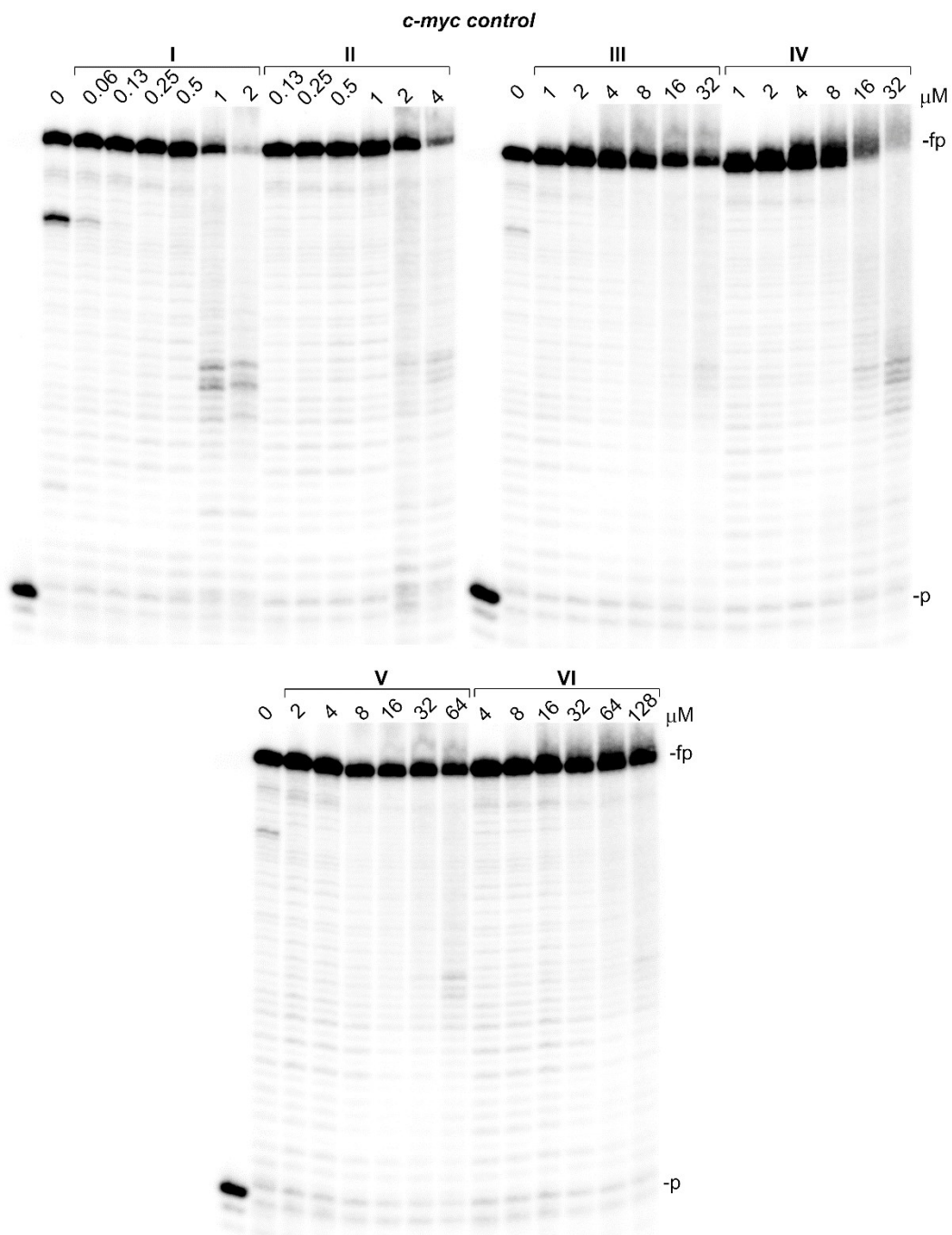


Fig. S3. Autoradiograms of 12% denaturing PAA gels for the *Taq* DNA polymerase stop assay on the *c-myc* ctrl template in the presence of increasing concentrations of **I-VI**. *p* and *fp* correspond to primer and full-length product, respectively.

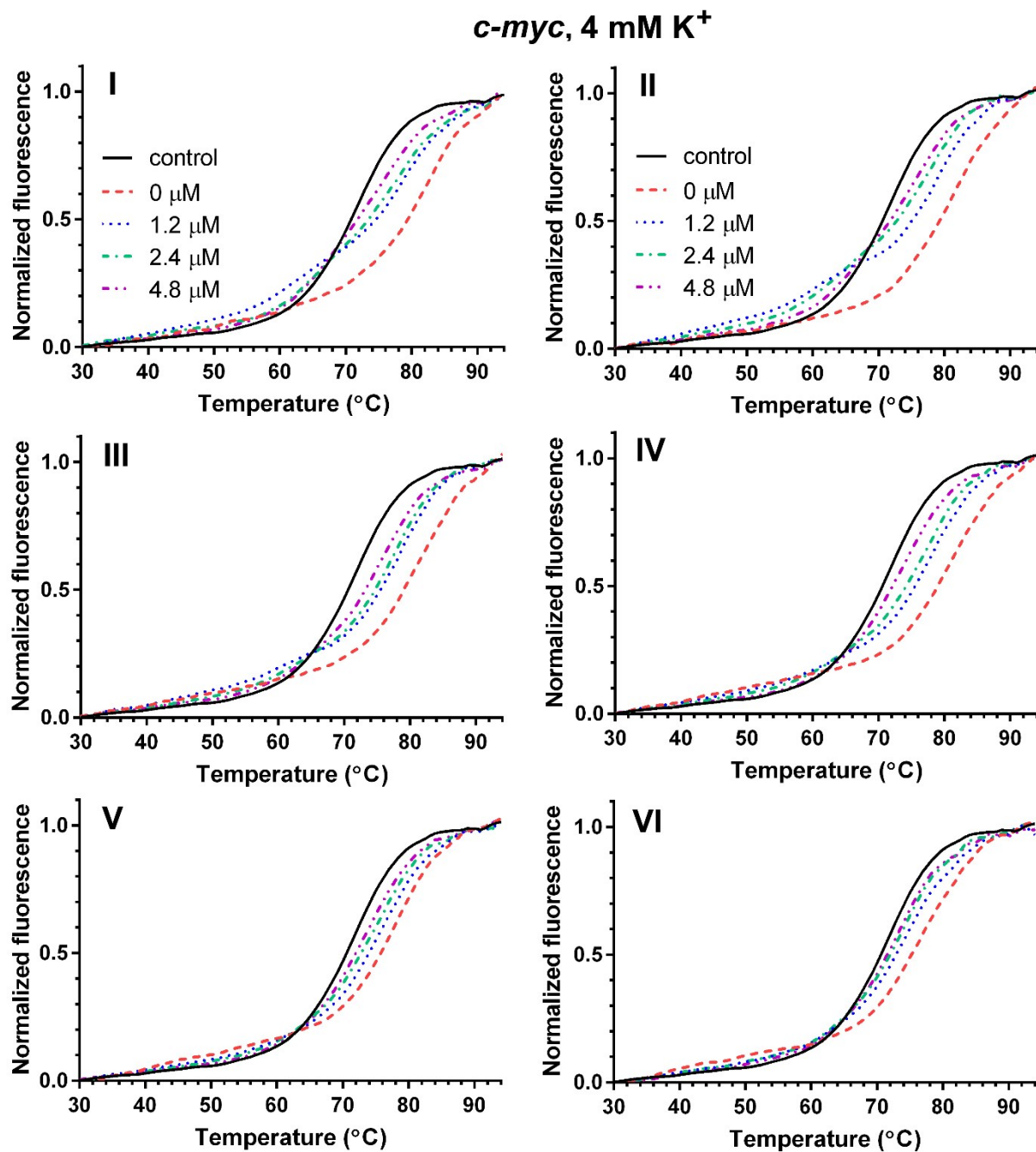


Fig. S4. Fluorescence melting curves for the fluorescent labeled *c-myc* G4 (0.4 μM) in the presence of 0.8 μM I-VI and increasing concentrations of the competitor duplex 26-ds. The buffer conditions were 4 mM potassium phosphate (pH 7) and the temperature gradient was 0.7 $^{\circ}\text{C}/\text{min}$. The concentrations of 26-ds are indicated in the Fig. 3.

***c-kit2*, 4 mM K⁺**

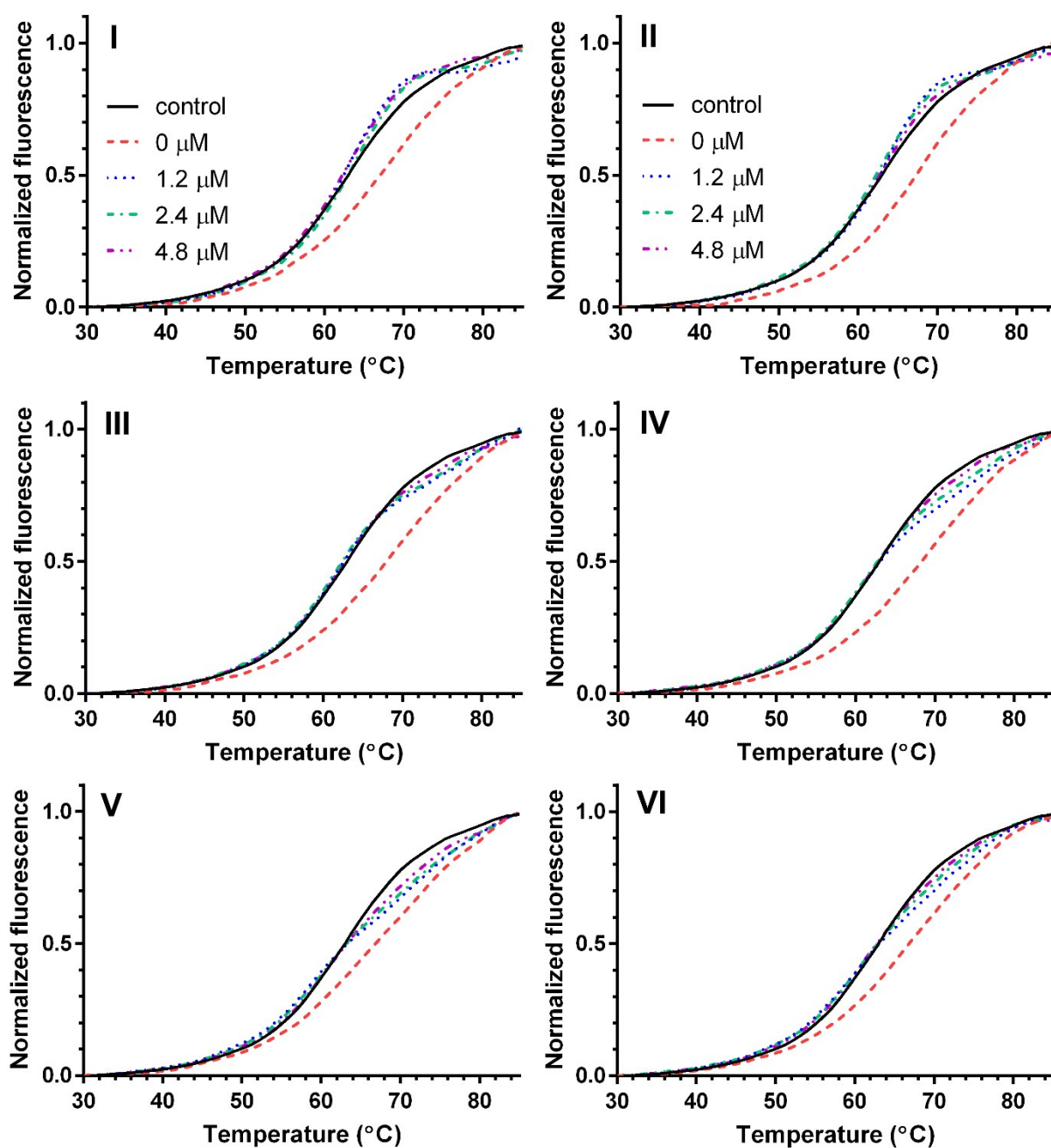


Fig. S5. Fluorescence melting curves for the fluorescent labeled *c-kit2* G4 (0.4 μM) in the presence of 0.8 μM **I-VI** and increasing concentrations of the competitor duplex 26-ds. The buffer conditions were 4 mM potassium phosphate (pH 7) and the temperature gradient was 0.7 °C/min. The concentrations of 26-ds are indicated in the Fig. 3.

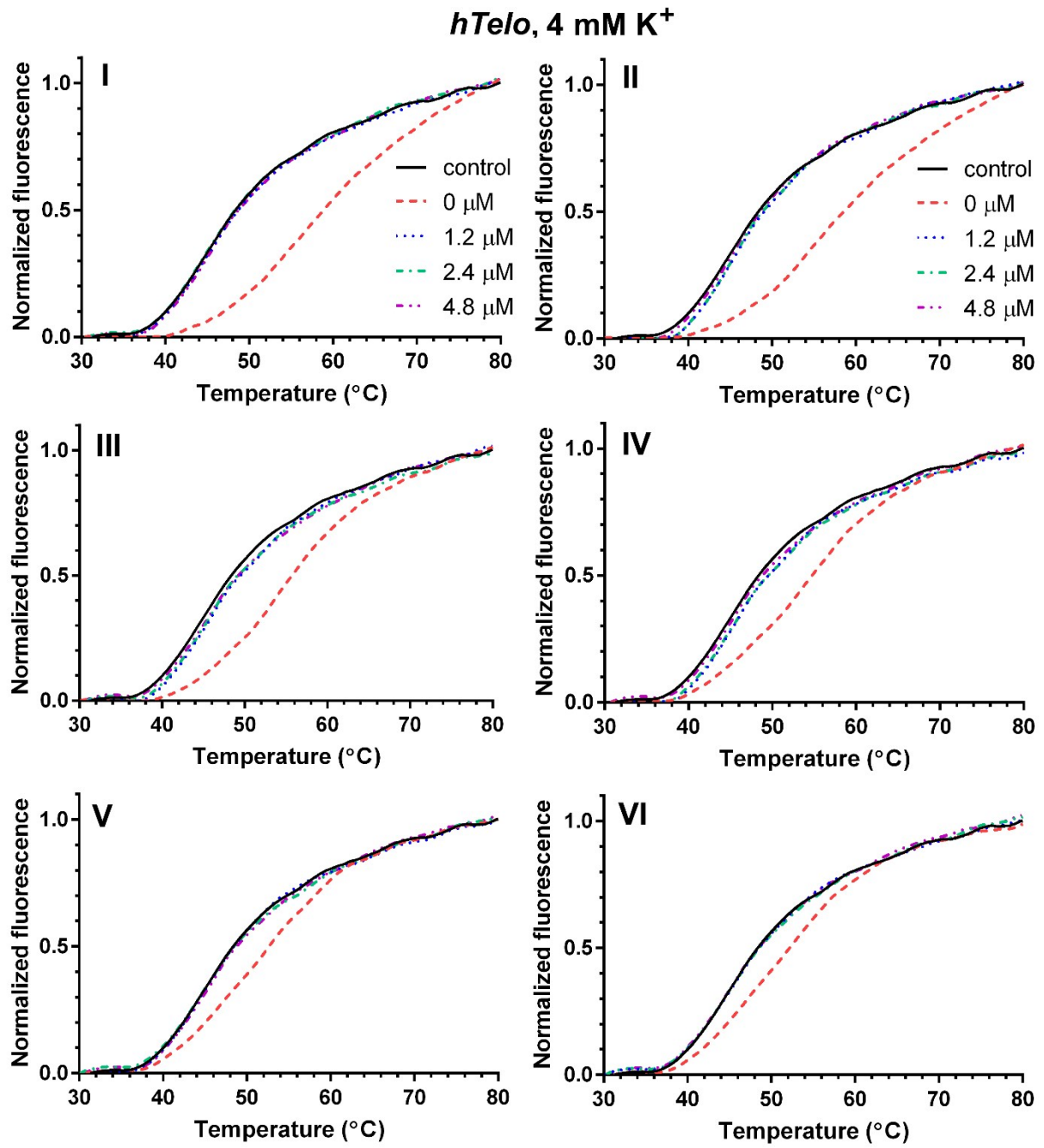


Fig. S6. Fluorescence melting curves for the fluorescently labeled *hTelo* G4 (0.4 μM) in the presence of 0.8 μM I-VI and increasing concentrations of the competitor duplex 26-ds. The buffer conditions were 4 mM potassium phosphate (pH 7) and the temperature gradient was 0.7 °C/min. The concentrations of 26-ds are indicated in the Fig. 3.

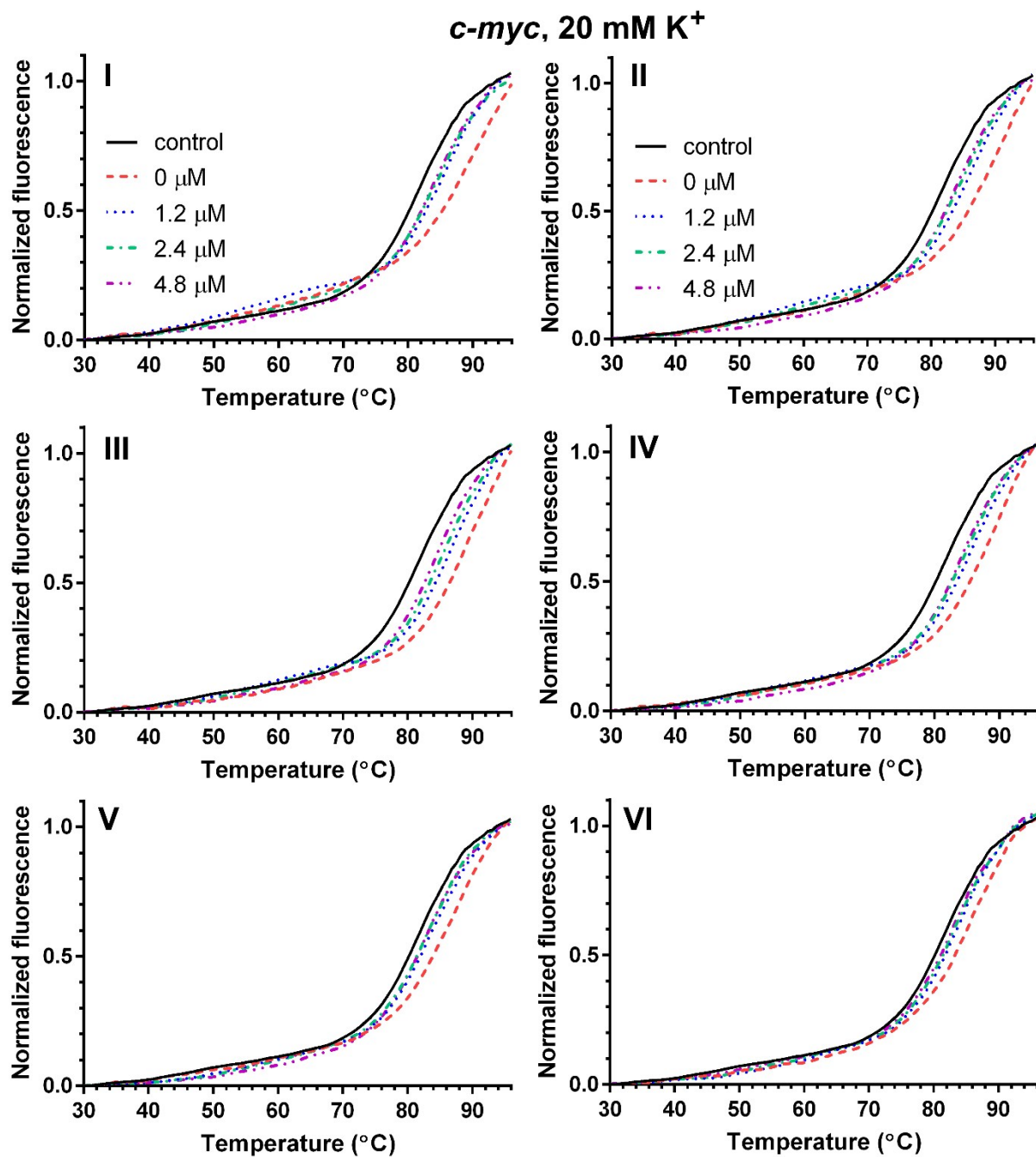


Fig. S7. Fluorescence melting curves for the fluorescent labeled *c-myc* G4 (0.4 μM) in the presence of 0.8 μM **I-VI** and increasing concentrations of the competitor duplex 26-ds. The buffer conditions were 10 mM potassium phosphate (pH 7) and 10 mM KCl and the temperature gradient was 0.7 °C/min. The concentrations of 26-ds are indicated in the Fig. 3.

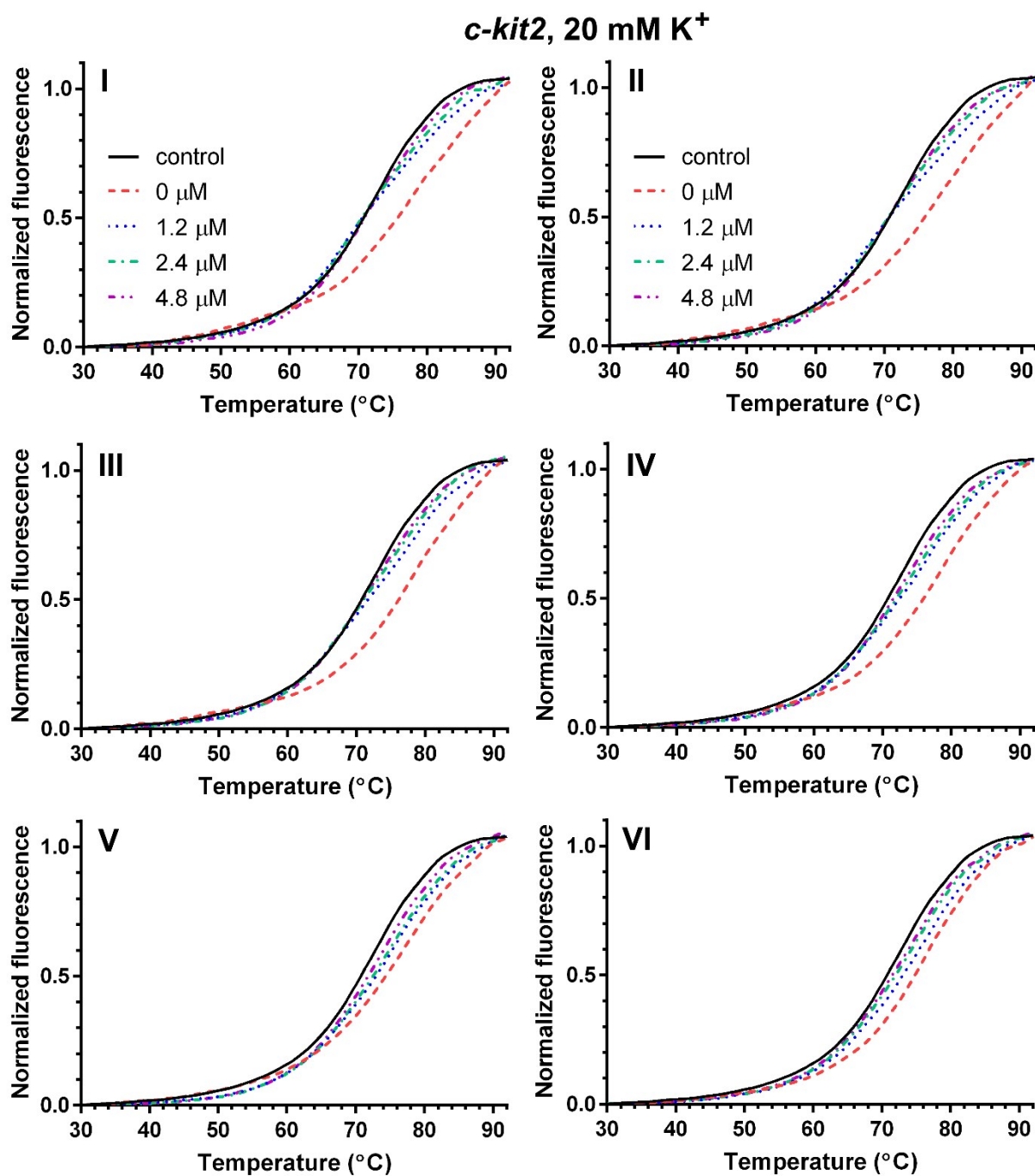


Fig. S8. Fluorescence melting curves for the fluorescent labeled *c-kit2* G4 (0.4 μM) in the presence of 0.8 μM **I-VI** and increasing concentrations of the competitor duplex 26-ds. The buffer conditions were 10 mM potassium phosphate (pH 7) and 10 mM KCl and the temperature gradient was 0.7 °C/min. The concentrations of 26-ds are indicated in the Fig. 3.

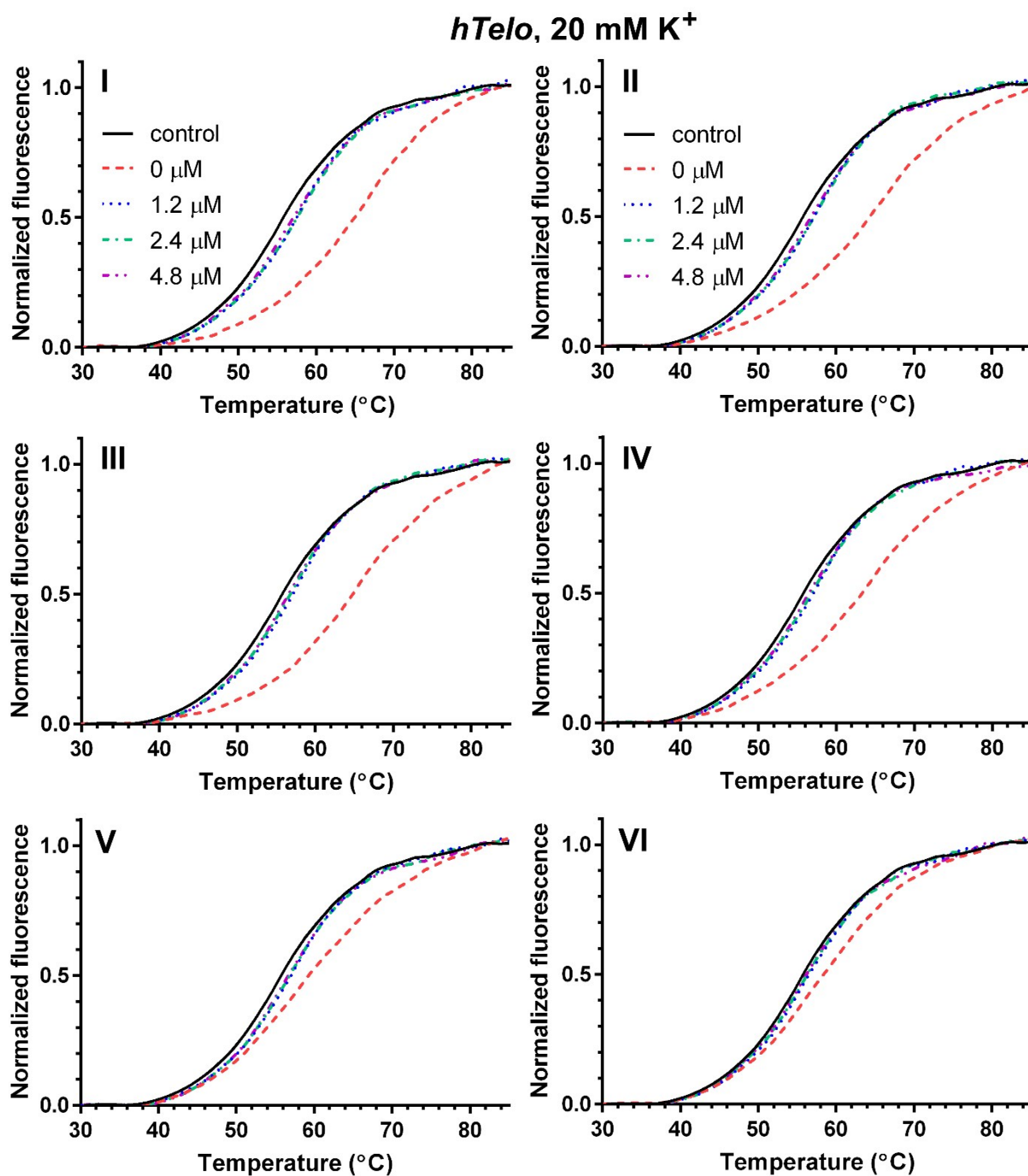


Fig. S9. Fluorescence melting curves for the fluorescently labeled *hTelo* G4 (0.4 μM) in the presence of 0.8 μM I-VI and increasing concentrations of the competitor duplex 26-ds. The buffer conditions were 10 mM potassium phosphate (pH 7) and 10 mM KCl and the temperature gradient was 0.7 $^{\circ}\text{C}/\text{min}$. The concentrations of 26-ds are indicated in the Fig. 3.

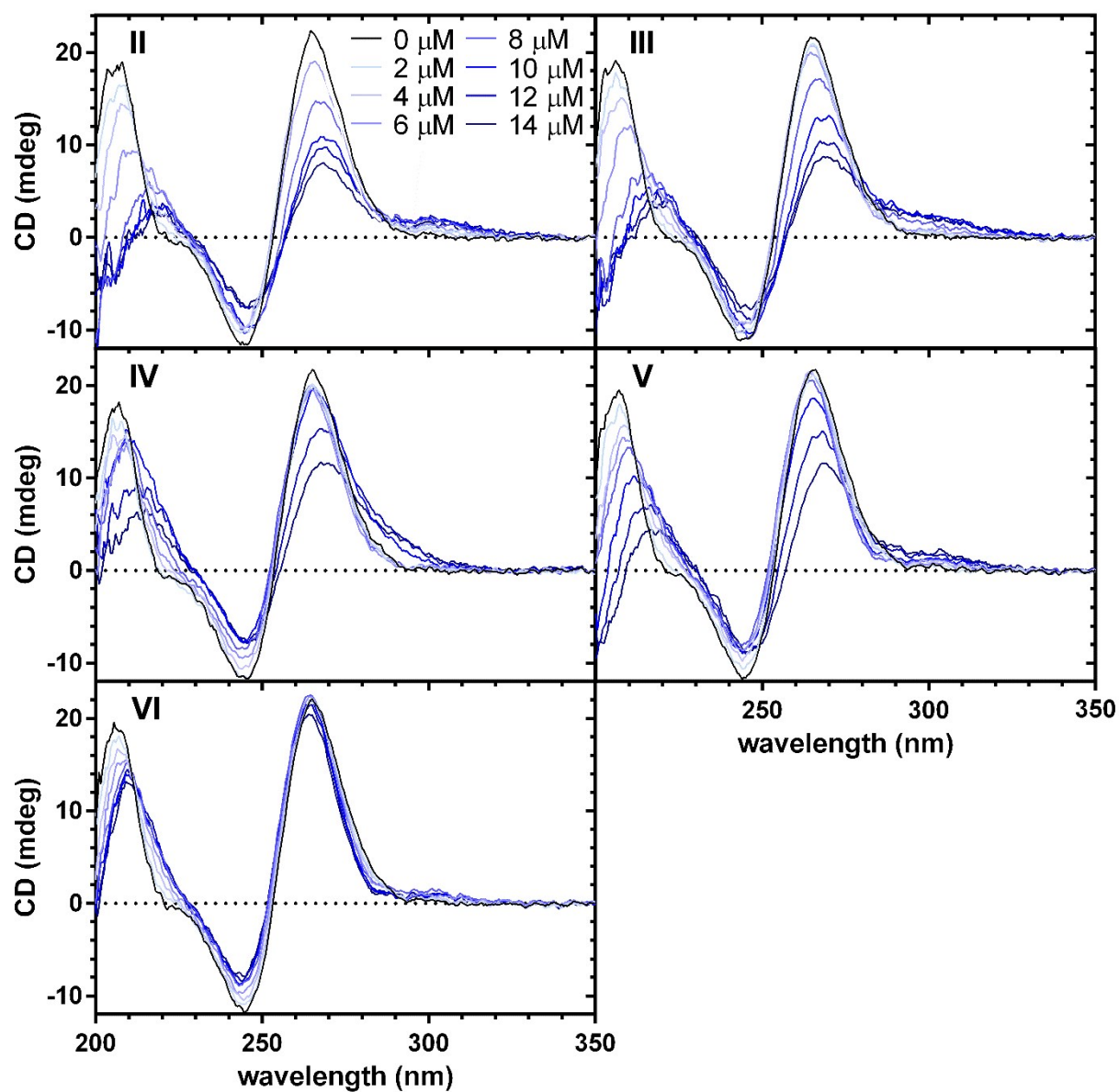


Fig. S10. CD spectra of 2.5 μM *c-myc* G4 in the presence of increasing concentrations of **II-VI**. The concentrations of **II-VI** are indicated in the Fig. 4A. The buffer conditions were 10 mM potassium phosphate (pH 7) and 30 mM KCl.

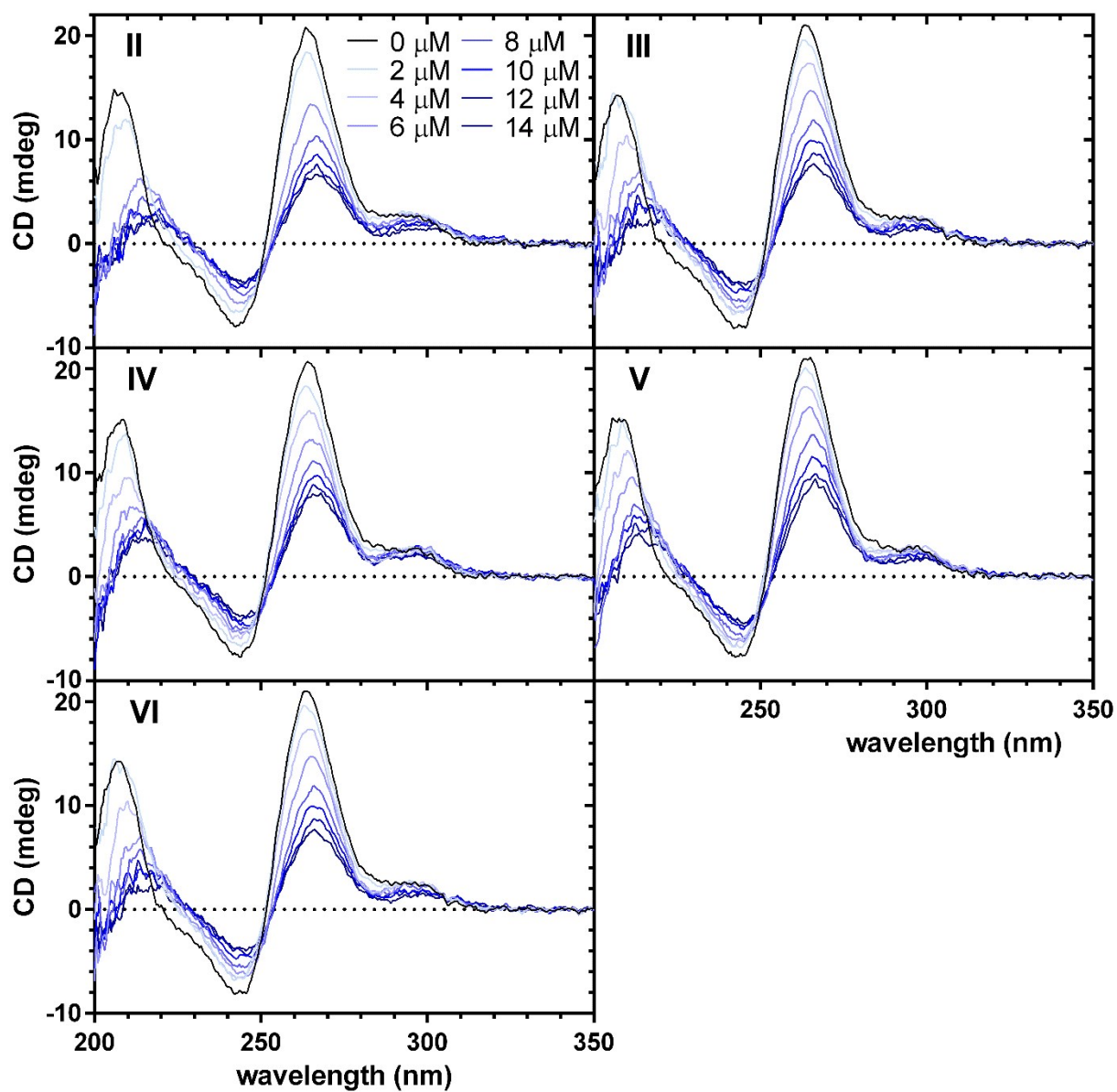


Fig. S11. CD spectra of 2.5 μM *c-kit2* G4 in the presence of increasing concentrations of **II-VI**. The concentrations of **II-VI** are indicated in the Fig. 4A. The buffer conditions were 10 mM potassium phosphate (pH 7) and 30 mM KCl.

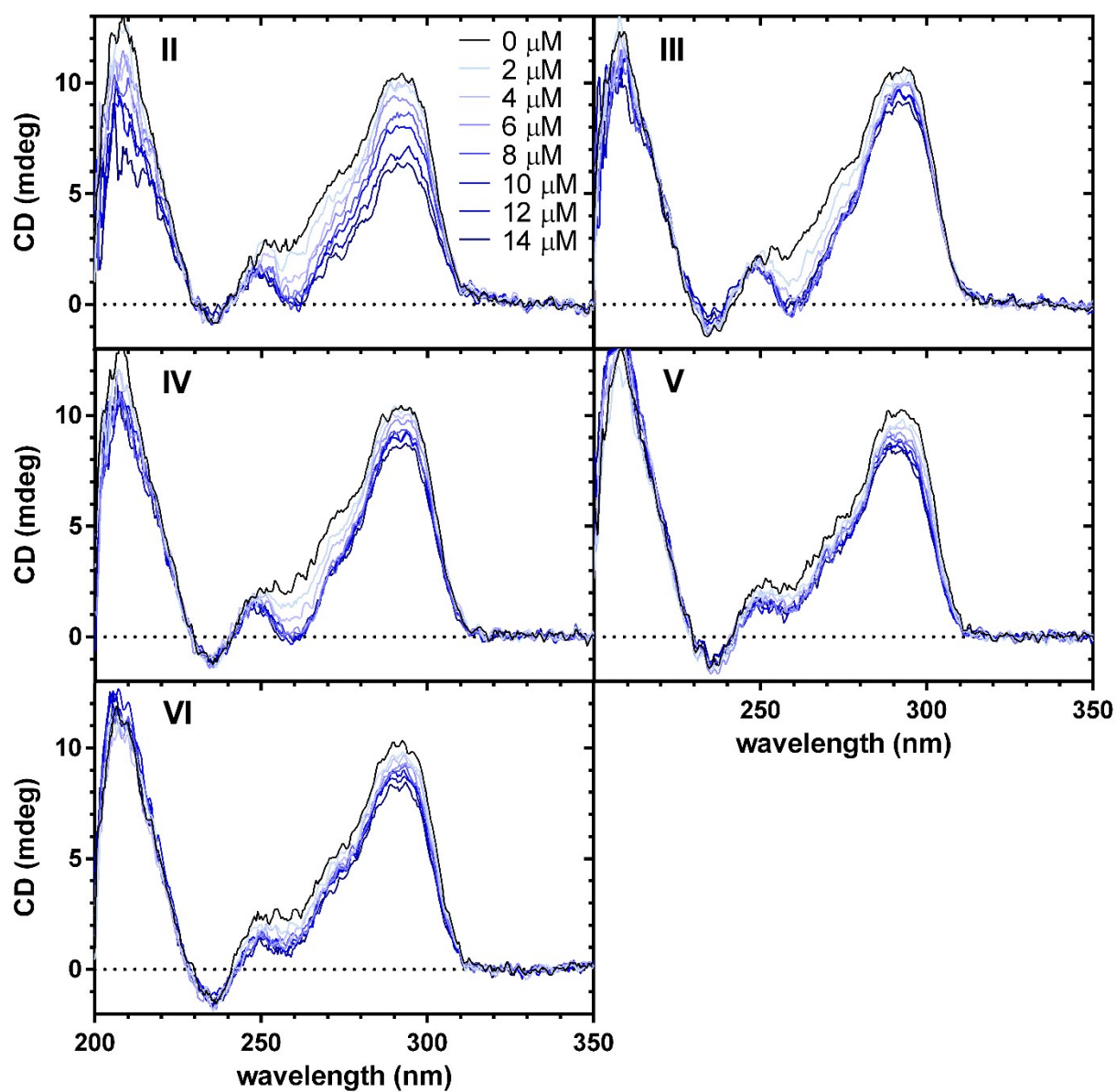


Fig. S12. CD spectra of 2.5 μM *hTelo* G4 in the presence of increasing concentrations of **II-VI**. The concentrations of **II-VI** are indicated in the Fig. 4A. The buffer conditions were 10 mM potassium phosphate (pH 7) and 30 mM KCl.

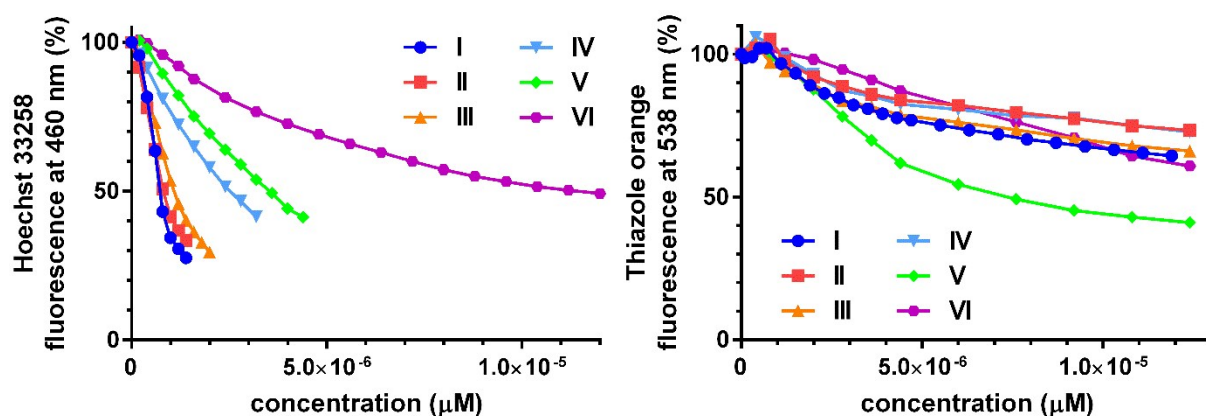


Fig. S13. Fluorescence response of the mixture of 0.25 μM *c-myc* G4 and 0.25 μM Hoechst 33258 (left panel), or TO (right panel) in the presence of increasing concentrations of **I-VI**. The buffer conditions were 10 mM potassium phosphate buffer (pH 7) and 30 mM KCl.

Table S1. Antiproliferative effects of the investigated SI-PPCs expressed as IC_{50} [μM]^[a] as determined with MTT assay after a 72 h treatment

	MDA-231	HCT116
Tetraplatin NC (I)	7 ± 1	3.4 ± 0.9
Triplatin NC (II)	12 ± 2	5.9 ± 0.9
Diplatin NC (IV)	41 ± 7	20 ± 4
Triplatin NC-A (III)	60 ± 10	28 ± 5
AH-59 (V)	140 ± 20	69 ± 4
AH-64 (VI)	> 200	170 ± 20

^[a] The results are expressed as mean values \pm SD from three independent measurements.